ELSEVIER

Sensors and Actuators A 57 (1996) 153–157

SENSORS AND ACTUATORS A PHYSICAL

The VAMP — a new device for handling liquids or gases

M. Stehr, S. Messner, H. Sandmaier, R. Zengerle *

Hahn-Schickard-Gesellschaft, Institut für Mikro- und Informationstechnik, Wilhelm-Schickard-Straße 10, D-78052 Villingen-Schwenningen, Germany

Abstract

We present a new device, the VAMP, which is both an active microvalve and a forward- and reverse-working micropump (VAMP = Valve And MicroPump). Driven by a d.c. voltage, the VAMP operates in its valve mode and is able to control fluid flow in both directions. Driven by a square wave or a sinusoidal voltage, the VAMP operates in its pump mode and is able to pump fluids in both directions. The direction of fluid transport can be changed by varying the driving frequency of the actuator. We discuss two new mechanisms, which in combination are responsible for this frequency-dependent pump effect. The VAMP has been successfully tested for liquids (water, oil) and air. Using water we have achieved maximum pump rates of more than 2000 $\mu l\ min^{-1}$ in the forward direction and 1200 $\mu l\ min^{-1}$ in the reverse direction. The maximum back pressure is 17 kPa (1.7 mH_2O) at a supply voltage of 200 V. Pumping air, we have achieved a maximum flow rate of 8000 $\mu l\ min^{-1}$ in both directions. The VAMP has been manufactured in a small-lot production and is now available for industrial evaluation.

Keywords: Micropumps; Pumps; Microvalves; Actuators; Microelectromechanical systems (MEMS); Microfluidics

1. Introduction

Miniaturized diaphragm pumps usually consist of a periodically working diaphragm and two passive check valves [1–8] (or diffuser/nozzle elements [9,10]). The valves or the diffuser/nozzle elements direct the fluid from the inlet to the outlet port. Under certain conditions pumps containing check valves can work in both forward and reverse directions. This can be achieved by driving the pump with frequencies higher than the resonance frequency of the check valves in the fluid environment (2–6 kHz). In this case there is a phase shift between the valve opening and the pump chamber pressure driving the fluid [11]. The change of the pump direction is a very interesting feature in many fields of application (miniaturized chemical analysis systems, micro-dosing systems, etc.). Nevertheless, until now there have been several practical limitations for using micropumps in commercial fluid systems. The most important limitations are:

(i) the missing self-priming capacity of the pumps;
(ii) the missing fluid blocking in the forward direction;
(iii) the leakage of the check valves if unfiltered fluids are used;
(iv) the complexity of the pump structures, which makes fabrication difficult and expensive.

Most of these problems can be overcome by the VAMP, a new device which can be operated as an active microvalve or even as an active micropump. Two new pump mechanisms, the elastic buffer mechanism [12] and the variable gap mechanism [13], are important in order to understand the pump effect. These two basic mechanisms are discussed in the following two sections using special layout examples.

2. Elastic buffer mechanism

According to the first new mechanism, the device consists of a pump chamber, bounded by a pump diaphragm (displacement unit), two fluid ports and an elastic buffer element (Fig. 1). All these parts can be manufactured by silicon micromachining, for example. During stand-by, the device is operated as a microvalve and port 2 is blocked by the pump diaphragm. This can be achieved by driving the piezo-bimorph actuator by a negative d.c. voltage. By driving the displacement unit with a square-wave voltage, port 2 is

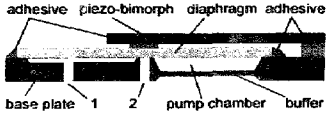

Fig. 1. Schematic of a micropump with the elastic buffer mechanism.

* Corresponding author. Fax: +49 7721 943 234. E-mail: zengerle@imit.uni-stuttgart.de.

PII S0924-4247(96)01349-0

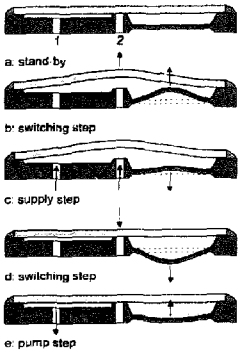

Fig. 2. Schematic for demonstration of the elastic buffer mechanism.

opened and shut periodically while port 1 is open all the time. This leads to a pumping effect as shown in Fig. 2.

In a first step the displacement unit is switched within a very short time (< 1 ms) and the corresponding volume displacement of the diaphragm is compensated by the deformation of the elastic buffer (Fig. 2(b)). Due to the inertia of the fluid, the volume flow through the ports is negligible within the short switching time. In a second step, fluid is sucked in through both ports, driven by the relaxation of the buffer element (Fig. 2(c)). In the third step, port 2 is blocked within a very short time (< 1 ms) and again the corresponding volume displacement is compensated by the deformation of the elastic buffer (Fig. 2(d)). During the last step the relaxation of the buffer drives all the fluid through port 1 (Fig. 2(e)). This gives rise to a pumping effect (port 2 → port 1), because fluid is sucked in through both ports and pushed out only through port 1. The pump direction can be switched by driving the displacement unit with frequencies higher than a resonance frequency determined by the fluid and the buffer element [14]. In this case there is a phase shift between the movement of the buffer and the opening of port 2. A typical resonance frequency is in the range 30–150 Hz, as tests have shown. These frequencies are much lower than the resonance frequency of passive check valves as described in Refs. [7] and [11] (800–2000 Hz).

If compressible fluids have to be pumped (e.g., air), the fluid itself can be used as a buffer. In this case a mechanical buffer structure (diaphragm) as depicted in Figs. 1 and 2 is not necessary.

3. Variable gap mechanism

According to the second new mechanism an elastic buffer is completely unnecessary (Fig. 3). The pumping effect can be explained by calculating the volume flow through port 2

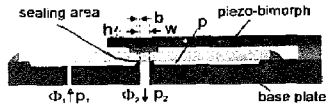

Fig. 3. Schematic of a micropump with the variable gap mechanism.

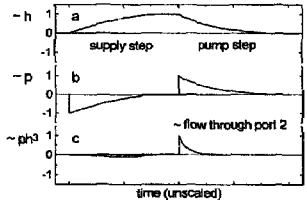

Fig. 4. Schematic for demonstration of the variable gap mechanism.

and integrating it during a pump cycle. Assuming laminar conditions, the volume flow through port 2 is given by

$$\Phi_2 = \frac{1}{3}\frac{wh^3(p - p_2)}{\eta b} \qquad (1)$$

where p_1, p_2 and p correspond to the hydrostatic pressures in the fluid channels 1 and 2 and in the pump chamber. η is the dynamic viscosity of the fluid, w denotes the width of fluid port 2, and h and b refer to the height and the length of the gap between the pump diaphragm and the sealing area of port 2.

When the piezo-bimorph actuator is driven by a pulsed d.c. voltage and the pump chamber is completely filled with liquid, the transient behaviour of h and p, respectively, is depicted in Fig. 4(a) and (b). The variable gap mechanism can be divided into two steps, a supply step and a pump step. During the opening of port 2 (supply step) there is a low pressure in the pump chamber (Fig. 4(b)) and the gap height h is increasing (Fig. 4(a)). During the closing of port 2 (pump mode) there is an overpressure in the pump chamber (Fig. 4(b)) and the gap height h is decreasing (Fig. 4(a)). The factor ph^3 is a measure of the fluid flow through port 2 and is depicted in Fig. 4(c). Integrating a pump cycle, it can be seen that there is a net fluid flow directed from port 1 to port 2. This is just the opposite direction to that of the elastic buffer mechanism.

4. Fabrication

For experimental analysis, several different types of VAMP have been fabricated. All devices contain a base plate made of Perspex and a bossed diaphragm made of micromachined silicon. The bossed diaphragm, base plate and piezo-bimorph actuator were assembled by using adhesives (Fig. 5). Tubes were connected to the base plate by MINSTAC 062 fittings. The layouts tested differ in the fabrication and geometry of the fluid ports 1 and 2 as well as in the stiffness of the bossed diaphragm. It is important to mention

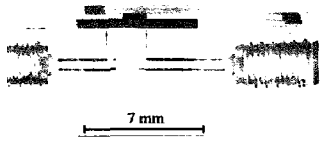

Fig. 5. Photograph of a device (type A).

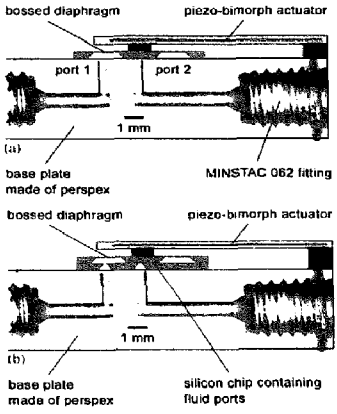

Fig. 6. Schematics of different layouts: (a) devices corresponding to type A; (b) devices corresponding to type B.

that neither type A nor type B devices contain special buffer elements as depicted in Figs. 1 and 2. However, in both cases the bossed diaphragm is working as a buffer too. Thus, in any given device, the resulting pump behaviour is always a superimposition of both the elastic buffer and variable gap mechanisms, although typically one of the two mechanisms predominates.

For devices corresponding to type A (Fig. 6(a)) the fluid ports 1 and 2 have been made by drilling in the base plate (diameter 0.6 mm). Three different geometries of the diaphragm were tested (type A1, 7.3 mm × 7.3 mm × 0.020 mm; type A2, 5.3 mm × 5.3 mm × 0.025 mm; type A3, 5.3 mm × 5.3 mm × 0.018 mm). The boss width of all devices is 2.1 mm. Devices of type B (Fig. 6(b)) contain a second silicon chip with fluid ports manufactured by anisotropic etching of silicon. Different widths of fluid ports 1 and 2 were tested (type B1, 200 μm; type B2, 400 μm; type B3, 800 μm). All devices of type B contain a bossed diaphragm with the dimensions 5.3 mm × 5.3 mm × 0.018 mm (boss width 2.1 mm) The dependence of gap height h on driving voltage V for all types is depicted in Fig. 7. A variation in the stiffness of the bossed diaphragm can clearly be seen.

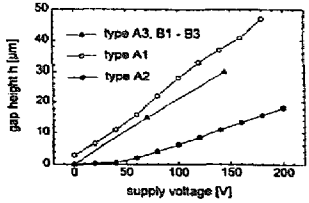

Fig. 7. Gap height h vs. supply voltage for different types.

5. Experimental results

The flow characteristic of the device, operated in the valve mode, is depicted in Fig. 8. Driven by a positive d.c. supply voltage, fluid flow is possible in both directions. Driven by a negative d.c. supply voltage, the flow is blocked. Due to the piezoelectric actuation principle, the power consumption is negligible (< 1 mW) in this operation mode. A small leakage of less than 0.5% of the open flow rate can be detected for devices corresponding to type A because the Perspex base plate is not flat enough to ensure perfect sealing. Due to the flatness of polished silicon, the sealing is significantly better for type B devices.

The frequency-dependent pump rate of the device when operated in the pump mode (pulsed d.c. voltage) is depicted in Fig. 9. For lower actuation frequencies the fluid transport is directed from port 1 to port 2 if liquids are pumped. This indicates that the variable gap mechanism is the predominant effect. For higher driving frequencies the pump direction changes. This is due to dynamic effects (for more details see Ref. [14]).

Very similar to other micropumps, there is nearly a linear dependence between pump rate and hydrostatic back pressure

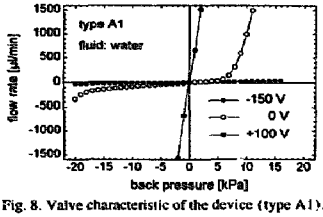

Fig. 8. Valve characteristic of the device (type A1).

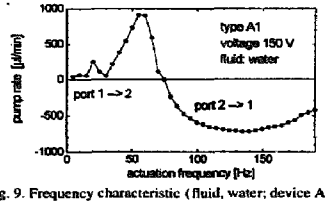

Fig. 9. Frequency characteristic (fluid, water; device A1).

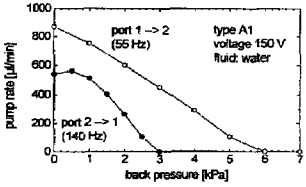

Fig. 10. Back-pressure characteristic (fluid, water; device A1).

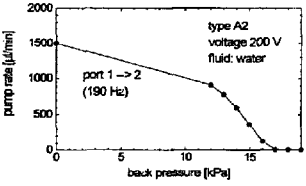

Fig. 11. Back-pressure characteristic (fluid, water; device A2).

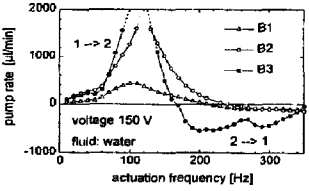

Fig. 12. Frequency characteristics for different types of devices (fluid, water).

working against the flow direction (Fig. 10). The maximum back pressures in forward and reverse directions are 6 and 3 kPa for type A1 devices at a supply voltage of 150 V. The maximum back pressure can be increased by increasing either the stiffness of the diaphragm (type A2) and/or the amplitude of the supply voltage (Fig. 11). A maximum back pressure of 17 kPa has been achieved for a type A2 device at a supply voltage of 200 V.

The variation of the width w of the fluid ports 1 and 2 has been studied on type B devices. It can be clearly seen from Fig. 12 that the maximum pump rate can be increased by larger fluid ports. The influence of the kinematic viscosities of liquids on the frequency-dependent pump characteristic have been studied on a type A3 device. The pump rate decreases with increasing viscosity as depicted in Fig. 13. A maximum pump rate of 20 μl min^{-1} has been achieved for a kinematic viscosity of 22 mm^2 s^{-1}. This pump rate is high enough for the dosage of lubrication oils, for example.

The devices (type A and B) have additionally been tested for air. Due to its compressibility, air works as an elastic buffer and thus we obtain the pump characteristic depicted in Fig. 14. It is very significant that the frequencies for pumping

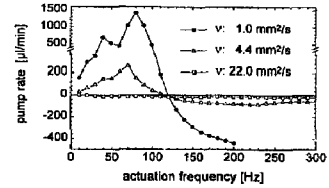

Fig. 13. Frequency characteristics for different kinematic viscosities of liquids (device A3; voltage, 150 V; water, $\nu = 1$ mm^2 s^{-1}; oil 1, $\nu = 4.4$ mm^2 s^{-1}; oil 2, $\nu = 22.0$ mm^2 s^{-1}).

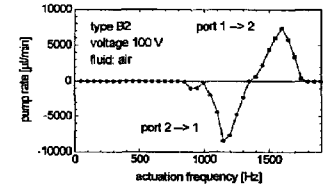

Fig. 14. Frequency characteristic (fluid, air; device B2).

gases (1–2 kHz) are much higher than the frequencies for pumping liquids (10–200 Hz). However, the most important effect is that the gas transport at lower frequencies is directed from port 2 to port 1. This contrasts with the behaviour for liquids and indicates that the elastic buffer mechanism dominates the variable gap mechanism when gases are pumped.

6. Self priming

Some of the published micropumps are able to pump both liquids and gases. Nevertheless, self priming of these pumps with liquids has never been reported. On the contrary, priming of micropumps is quite often very laborious, especially when they include passive check valves. The reason is that capillary forces prevent the flow when the liquid surface reaches the movable valve part. As has been calculated in Ref. [1], a large force is needed to overcome the capillary forces. The force generated by the driving units of micropumps is not large enough. This is due to two effects:

(i) the force generated by the driving unit is converted to a gas pressure inside the pump chamber;

(ii) the gas pressure inside the pump chamber is converted to a force acting on the microvalve.

Both conversions in typical micropump designs are combined with large losses due to the compressibility of the air inside the pump chamber and due to the small active area of a check valve (e.g. Ref. [7], 0.4 mm × 0.4 mm). Using the devices discussed in this paper, there is no loss caused by the effects (i) and (ii), because the whole force generated by the piezo-bimorph actuator is used directly to open port 2 (Fig. 3).

Nevertheless, the pump chamber geometry of type A and B devices is unsuited to ensure self priming due to the large peripheral cavities. As a next step the height of the pump chamber has to be optimized in such a way that the capillary forces inside the pump chamber support the priming procedure when the fluid level enters the chamber. In a first crude experiment, the bossed diaphragm of a type A device (Fig. 6(a)) was mounted upside down on top of the base plate leading to a pump chamber height in the micrometre range. In this experiment the pump chamber was instantly completely filled with water when the fluid level reached port 2. It has been proved that self priming of the VAMP element with liquids is very reproducible for this new design if the pump chamber is dry. However, if there is any remaining liquid in it, the behaviour of the capillary forces changes significantly and the self priming of the device fails. Further experiments are being done to find an optimum for the pump chamber height. These experiments are based on the design depicted in Fig. 3.

7. Conclusions

We have presented a new device. Driven by a d.c. voltage, the VAMP works as an active valve controlling fluid flow in both directions. Driven by a square wave or a sinusoidal voltage, the VAMP is able to pump liquids and gases in the forward and reverse direction, respectively. The device is very important for miniaturized fluid systems where several fluids have to be handled and delivered in different directions, such as in chemical analysis systems. In this case cross-talk between the different fluid channels can be excluded by the active blocking of the VAMP. The construction of the device is simple. It consists of a flexible diaphragm, a simple base plate with two orifices and a piezo-bimorph actuator. In addition, it should be possible to manufacture the VAMP completely of plastic, e.g., by injection moulding. This would make fabrication cheap and simple. The self priming of the VAMP with liquids has been confirmed under certain conditions in the laboratory. A reproducible priming procedure will be developed and stabilized in further experiments. This will significantly facilitate the handling of micropumps in microfluid systems. The VAMP has been manufactured in a small-lot production and is now available for industrial evaluation.

References

[1] P. Gravesen, J. Branebjerg and O.S. Jensen, Microfluidics — A review, *Micro Mechanics Europe, Neuchâtel, Switzerland, 1993*, pp. 143–164.

[2] H.T.G. Van Lintel, F.C.M. Van de Pol and S. Bouwstra, A piezoelectric micropump based on micromachining of silicon, *Sensors and Actuators, 15* (1988) 153–167.

[3] F.C.M. Van de Pol, H.T.G. Van Lintel, M. Elwenspoek and J.H.J. Fluitman, A thermo-pneumatic micropump based on micro-engineering techniques, *Sensors and Actuators, A21–A23* (1990) 198–202.

[4] S. Shoji, S. Nakagawa and M. Esashi, Micropump and sample injector for integrated chemical analyzing systems, *Sensors and Actuators, A21–A23* (1990) 189–192.

[5] R. Zengerle, W. Geiger, M. Richter, J. Ulrich, S. Kluge and A. Richter, Application of micro diaphragm pumps in microfluid systems, *Proc. Actuator '94, Bremen, Germany, 15–17 June, 1994*, pp. 25–29.

[6] B. Büstgens, W. Bacher, W. Menz and W.K. Schomburg, Micropump manufactured by thermoplastic molding, *Proc. MEMS '94, Osio, Japan, 1994*, pp. 18–21.

[7] R. Zengerle, J. Ulrich, S. Kluge, M. Richter and A. Richter, A bidirectional silicon micropump, *Sensors and Actuators A, 50* (1995) 81–86.

[8] J. Döpper, M. Clemens, W. Ehrfeld, K.-P. Klämper and H. Lehr, Development of low-cost injection moulded micropumps, *Proc. Actuator '96, Bremen, Germany*, in press.

[9] A. Olson, P. Enokson, G. Stemme and E. Stemme, An improved valveless pump fabricated using deep reactive ion etching, *Proc. MEMS '96, San Diego, CA, USA, 1996*, pp. 479–482.

[10] T. Gerlach and H. Wurmus, Working principle and performance of the dynamic micropump, *Proc. MEMS '95, Amsterdam, The Netherlands, 1995*, pp. 221–226.

[11] J. Ulrich and R. Zengerle, Static and dynamic flow simulation of a KOH-etched microvalve using the finite-element method, *Sensors and Actuators A, 52–54* (1996) 379–385.

[12] M. Stehr, Fluidpumpe, *German and international patents pending*.

[13] R. Zengerle, M. Stehr and S. Messner, Fluidpumpe, *German and international patents pending*.

[14] J. Ulrich, M. Stehr and R. Zengerle, Simulation of a bidirectional pumping microvalve using FEM, accepted for publication in *Proc. Eurosensors '96, Leuven, Belgium*.